Int. J. Heat Mass Transfer. Vol. 5, pp. 35–57. Pergamon Press 1962. Printed in Great Britain.

MASS TRANSFER THROUGH LAMINAR BOUNDARY LAYERS—7. FURTHER SIMILAR SOLUTIONS TO THE *b*-EQUATION FOR THE CASE $B = 0$

H. L. EVANS

Commonwealth Scientific and Industrial Research Organization,
Division of Food Preservation, P.O. Box 43, Ryde, New South Wales, Australia

(*Received* 8 *February*, 1961)

Abstract—The present paper is concerned with uniform property, laminar boundary-layer flows when no mass passes through the interface. Similar solutions to the velocity equation for this case were found in the literature; these were given to high accuracy and covered the range of decelerated and moderately accelerated main-streams. The solutions are first expressed in the form adopted in the first papers of the present series, and are then used in evaluating the wall gradient for the *b*-boundary layer (i.e. the Nusselt number in similar co-ordinates). The series expansions for obtaining this wall gradient when the Prandtl/Schmidt number σ is large, already given in Paper 3(a), have been recalculated to improve their accuracy. A table of values of the wall gradient covers the range of σ from 0·0001 to 1000; it can readily be calculated in both directions outside this range. Some functions obtained from the wall gradient are plotted and discussed.

NOTATION

Where the quantities in the following list have dimensions these are given in brackets, otherwise they are dimensionless.

- a_q, coefficients occurring in equation (49) and defined in equations (51) to (59);
- A_r, coefficients occurring in equation (45) and defined in equation (47);
- b, conserved fluid property in dimensionless form defined in equation (19); discussed in Paper 3;
- b'_0, gradient of b in the fluid adjacent to the interface; see equation (24);
- B, value of b in the main-stream; it is the driving force for mass transfer; see equation (23);
- C, constant occurring in equation (5);
- d, dimensionless distance occurring in equation (41); it is the smallest convenient value of the similar co-ordinate η at which the flow can be regarded as inviscid;
- D, abbreviation for $\beta/(f''_0)^{4/3}$ which occurs in the expressions for the coefficients a_q;
- E, integral defined by equation (45) evaluated numerically from equation (49);
- E_2, correction factor defined by equation (34) tabulated in Table 1;
- f, dimensionless stream function; defined by equation (11);
- $f_0, f''_0, f^{(r)}_0$, values of f and its derivatives at the interface;
- F_2, function, defined in equation (33), giving rate of growth of the momentum thickness δ_2;
- H_{12}, ratio of displacement thickness δ_1 to the momentum thickness δ_2;
- H_{24}, ratio of momentum thickness δ_2 to shear thickness δ_4;
- K, thermal diffusivity of the fluid for heat transfer or the diffusion coefficient of a mass component in the fluid mixture for mass transfer (ft^2/h);
- m, number occurring in equation (48) specifying terms in the expanded form of equation (45);
- n, constant occurring in equation (5);
- Nu, Nusselt number in terms of the distance x;
- P, any fluid property, expressed in suitable dimensionless form, which is conserved during transfer processes;

P_G, value of P in the main-stream;
P_S, value of P in the fluid at the interface;
P_T, value of P in the transferred substance (see Spalding [7]);
q, number specifying terms in equation (49);
r, number specifying terms in equation (47);
Re, local Reynolds number ($= u_G x/\nu$);
u, velocity component parallel to the interface (ft/h);
u_G, value of u in the main-stream (ft/h);
v, velocity component perpendicular to the interface (ft/h);
x, distance parallel to the interface measured from the start of the boundary layer (ft);
y, distance perpendicular to the interface measured from the interface towards the main-stream (ft).

Greek symbols
β, parameter occurring in the similar form of the velocity equation and defined in equation (12);
γ, fluid property called the exchange coefficient and defined as $K\rho$, (lb/ft h);
δ, any boundary-layer thickness associated with the velocity boundary layer (ft);
δ_1, displacement boundary-layer thickness; $= \int_0^\infty (1 - u/u_G)\, dy$, (ft);
δ_1^*, displacement thickness in terms of similar co-ordinates; defined in equations (27) and (37) for different similar co-ordinates;
δ_2, momentum boundary-layer thickness; $= \int^\infty (u/u_G)(1 - u/u_G)\, dy$, (ft);
δ_2^*, momentum thickness in similar co-ordinates; defined in equations (28) and (38) for different similar co-ordinates;
δ_4, shear boundary-layer thickness; $= u_G/(\partial u/\partial y)_{y=0}$, (ft);
δ_4^*, shear thickness in similar co-ordinates; an alternative expression for $1/f_0''$, but not used in the present paper;
Δ, any boundary-layer thickness associated with the b-boundary layer, (ft);
Δ_2, convection thickness; $= \int_0^\infty (u/u_G)(1 - b/B)\, dy$, (ft);
Δ_2^*, convection thickness in similar co-ordinates; defined by equation (68);
Δ_4 conduction thickness; $= B/(\partial b/\partial y)_{y=0}$, (ft);
Δ_4^*, conduction thickness in similar co-ordinates, defined by equation (67);
ζ, dimensionless stream function; defined by equation (7);
ζ_0, value of ζ in the fluid at the interface where $\xi = 0$;
η, dimensionless distance co-ordinate; defined by equation (10);
μ, dynamic viscosity of fluid (lb/ft h);
ν, kinematic viscosity of fluid; $= \mu/\rho$, (ft^2/h);
ξ, dimensionless distance co-ordinate; defined by equation (6);
ρ, density of fluid (lb/ft^3);
σ, Prandtl or Schmidt number of fluid; $= \nu/K$;
φ, integration variable used in Section 4.2; defined in equation (44);
ψ, stream function; defined by equation (3), (ft^2/h).

Subscripts
G, denotes fluid state in the main-stream;
0, denotes fluid state at the interface;
q, denotes terms in equation (49);
r, denotes terms in equation (45) like A_r in equation (47).

1. EARLIER PAPERS IN THE SERIES

1.1. *Introduction*

THE present series of papers is concerned with methods of calculating mass transfer rates for laminar boundary-layer flows when the fluid properties may be considered uniform throughout and internal dissipation of energy is negligible. Within these limitations, however, three important parameters associated with the problem are allowed to take values over as wide a range as it is practicable to cover. These are (a) the Prandtl/Schmidt number of the fluid, (b) the pressure gradient in the main-stream and (c) the mass transfer rate. Both inward and outward mass transfer through the interface are considered.

It has been shown in earlier papers that the problem of predicting mass transfer rates reduces to the simultaneous solution of two partial differential equations, (1) the velocity equation, which is concerned with the distribution in the boundary layer of purely mechanical quantities like velocity, momentum and shear stresses, and (2) the b-equation, which governs the distribution of other conserved fluid properties.

For a general type of problem, such as one where fluid flows over a surface on which the distribution of both pressure gradient and mass transfer rate are arbitrary, the latter quantity usually being unknown, solution of the equations presents a formidable task and is rarely attempted.

On the other hand the equations possess "similar" solutions in which the three parameters listed above may take any values, or combination of values, likely to be encountered in any practical problem. These "similar" solutions form the basis of methods of boundary-layer calculation which may be used for any boundary-layer flow. Although these general methods are approximate by nature they would be expected to give the order of accuracy required for most engineering and design purposes.

The first part of the problem to be solved therefore is to obtain continuous families of "similar" solutions at convenient, if possible regular, intervals in the three varying parameters. The second part is to devise suitable general methods of boundary-layer calculation and draw up appropriate tables and charts from the "similar" solutions for use with these methods.

1.2. *Summary of earlier papers*

The first two papers in the series, Spalding [1], Spalding and Evans [2], were concerned exclusively with the velocity equation, the first describing the relevant general method applicable to any boundary-layer flow with mass transfer, the second supplying the appropriate tables and charts for use with this method and derived from exact similar solutions.

Paper 3, Spalding and Evans [3], considered the b-equation. Only a few exact similar solutions to this equation could be found in the literature and these were tabulated. Other tables were also supplied from which approximate solutions could be obtained for ranges in the three parameters considered.

Paper 3a, Evans [4], which was also concerned with the b-equation, considered the case when B, the driving force for mass transfer, was zero and the Prandtl/Schmidt number σ was greater than 0·5. Series in inverse powers of σ were given from which the gradient at the interface for the b-boundary layer could be evaluated for any high value of σ and for a wide range of main-stream pressure gradient. Even for σ near unity the series gave good accuracy.

In Paper 6, Evans [5], methods were given for evaluating this gradient accurately if similar solutions to the velocity equation are known. A table of values of this gradient was also given for the case of zero main-stream pressure gradient covering wide ranges in the mass transfer rate and Prandtl/Schmidt number.

1.3. *How the present paper is related to preceding papers*

The present paper, like Paper 3a, Evans [4], is concerned with the case when the driving force for mass transfer is zero. The inclusion of the case of zero mass transfer in a series mainly devoted to methods of predicting mass transfer rates has already been justified in the earlier paper. Since writing that paper, however, developments have occurred which made it possible to extend the range in the parameters for which results could be obtained as well as to improve the accuracy.

Firstly, similar solutions to the velocity equation were found in the literature giving considerably higher accuracy than was available hitherto. These were particularly useful for decelerated flows, when separation conditions are approached, since in that region they were given at small intervals in the relevant parameter. Unfortunately, however, as they were largely confined to wedge-type flows, they did not include cases of very highly accelerated main-streams.

Secondly, a method was evolved for evaluating the wall gradient to the b-boundary layer accurately from solutions to the velocity equation. This method, which was described in Paper 6, could be used for any values of the three parameters mentioned above. The calculations were relatively short even for low values of the

Prandtl/Schmidt number; these cases had previously involved rather long calculations.

Thirdly, a computer became available for carrying out the necessary calculations. Apart from increasing the speed with which wall gradients could be evaluated, this allowed the use of more accurate formulae for numerical integration.

In many respects, therefore, the present paper supersedes Paper 3a, although most of the discussion contained in that paper will not be repeated here. On the other hand, since more accurate solutions to the velocity equation are now available, the series expansions used in that paper for evaluating the wall gradient for high values of the Prandtl/Schmidt number have been recalculated. In order to present these, therefore, a certain amount of repetition will be necessary.

2. THE "SIMILAR" FORM OF THE BOUNDARY-LAYER EQUATIONS

2.1. *The velocity equation*

When the fluid properties are uniform the equation of motion for the fluid in the boundary layer is:

$$u \frac{\partial u}{\partial x} + v \frac{\partial u}{\partial y} = u_G \frac{\mathrm{d}u_G}{\mathrm{d}x} + \nu \frac{\partial^2 u}{\partial y^2} \tag{1}$$

and the continuity equation is:

$$\frac{\partial u}{\partial x} + \frac{\partial v}{\partial y} = 0. \tag{2}$$

In these equations:

x = distance measured parallel to the interface from the start of the boundary layer,
y = distance measured from the interface and perpendicular to it towards the main-stream,
u = velocity component in the x-direction,
v = velocity component in the y-direction,
u_G = value of u in the main-stream, and
ν = kinematic viscosity of the fluid.

Equations (1) and (2) are combined by introducing the stream function ψ defined by:

$$u = \frac{\partial \psi}{\partial y}, \quad v = -\frac{\partial \psi}{\partial x} \tag{3}$$

so that equation (2) is automatically satisfied and equation (1) becomes:

$$\frac{\partial \psi}{\partial y} \cdot \frac{\partial^2 \psi}{\partial x \partial y} - \frac{\partial \psi}{\partial x} \cdot \frac{\partial^2 \psi}{\partial y^2} = u_G \frac{\mathrm{d}u_G}{\mathrm{d}x} + \nu \frac{\partial^3 \psi}{\partial y^3}. \tag{4}$$

It was shown in Paper 1, Spalding [1], that this equation has "similar" solutions when the main-stream velocity u_G obeys the equation:

$$\frac{\mathrm{d}u_G}{\mathrm{d}x} = C\, u_G^n \tag{5}$$

where C and n are constants. It was further shown that by introducing the transformation:

$$\xi = y \sqrt{\left(\frac{1}{\nu} \frac{\mathrm{d}u_G}{\mathrm{d}x}\right)} \tag{6}$$

$$\zeta = \frac{\psi}{u_G} \sqrt{\left(\frac{1}{\nu} \frac{\mathrm{d}u_G}{\mathrm{d}x}\right)} \tag{7}$$

in which ξ is the new independent variable and the stream function ζ is a function of ξ only, equation (4) reduces to the ordinary differential equation:

$$\frac{\mathrm{d}^3\zeta}{\mathrm{d}\xi^3} + \left(1 - \frac{n}{2}\right) \zeta \frac{\mathrm{d}^2\zeta}{\mathrm{d}\xi^2} + 1 - \left(\frac{\mathrm{d}\zeta}{\mathrm{d}\xi}\right)^2 = 0. \tag{8}$$

The boundary conditions associated with this equation for the case when mass flows through the interface are:

$$\left.\begin{aligned} &\xi = 0, \left(\frac{\mathrm{d}\zeta}{\mathrm{d}\xi}\right) = 0, \quad \zeta = \zeta_0 \\ &\xi \to \infty, \left(\frac{\mathrm{d}\zeta}{\mathrm{d}\xi}\right) \to 1. \end{aligned}\right\} \tag{9}$$

The present series of papers is concerned with positive, zero and negative values of ζ_0, the value of the stream function at the interface, although in the present paper interest is confined to the case when this, or its counterpart in different similar co-ordinates, is zero. As later formulae will contain this quantity it is given a general symbol in equation (9).

Equation (8) with boundary conditions (9) govern the velocity distribution in the boundary layer for "similar" flows. This form of the equation has been included here since it will be necessary to refer to it in Section 2.2. Throughout the present series of papers, however, a form has been used which more commonly occurs in publications on laminar boundary-layer theory. This is obtained by using, instead of the variables defined in equations (6) and (7), the variables:

$$\eta = y \sqrt{\left(\frac{1}{\nu\beta} \cdot \frac{\mathrm{d}u_G}{\mathrm{d}x}\right)} \tag{10}$$

$$f = \frac{\psi}{u_G} \sqrt{\left(\frac{1}{\nu\beta} \cdot \frac{\mathrm{d}u_G}{\mathrm{d}x}\right)} \tag{11}$$

where β is a parameter related to the parameter n introduced in equation (5) by:

$$\beta = \frac{1}{(1 - n/2)}. \tag{12}$$

The equation for "similar" solutions to equation (4) then takes the form:

$$f''' + ff'' + \beta(1 - f'^{\,2}) = 0 \tag{13}$$

with the boundary conditions:

$$\left.\begin{aligned} &\eta = 0, \quad f = f_0, \quad f' = 0 \\ &\eta \to \infty, \quad f' \to 1. \end{aligned}\right\} \tag{14}$$

In equations (13) and (14) the primes denote differentiation with respect to the independent variable η, and again interest in the present paper is largely confined to the case when f_0 in equation (14), the counterpart of ζ_0 in equation (9), is zero.

2.2. *The "similar" velocity equation when $f_0 = 0$ and β is infinite*

As was stated in the first two papers of the present series, solutions to equation (13) with boundary conditions (14) are required for all real values of the parameter β.

Considering only the case $f_0 = 0$, equation (13) is quite suitable for evaluating solutions numerically for values of β from $-0{\cdot}198838$, when the velocity layer separates (i.e. the wall shear becomes zero), to high positive values. It was shown in Paper 2, Spalding and Evans [2], that for large negative values of β the appropriate equation is obtained from equation (13) by replacing both the independent variable η and the dependent variable f by pure imaginary quantities.

The case $n = 2$ in equation (5) forms the boundary between real and imaginary zones. At this value of n, equation (12) shows that β undergoes an infinite discontinuity, being large and positive on the real side (when $n < 2$) and large and negative on the imaginary side ($n > 2$). For this reason the transformation given in equations (10) and (11) cannot be used and therefore numerical solutions cannot be evaluated from equation (13).

By examining equation (5), however, it may be seen that the case $n = 2$ corresponds to flow near a point sink. If two streamlines in such a flow are regarded as the walls of a converging channel this case describes the boundary layer along these walls. The appropriate differential equation is well known, see for example Pai [6], and is readily obtained from equation (8), since when no mass flows through the wall ($\zeta_0 = 0$) the second term on the left-hand side is zero. The equation is therefore:

$$\frac{\mathrm{d}^3\zeta}{\mathrm{d}\xi^3} + 1 - \left(\frac{\mathrm{d}\zeta}{\mathrm{d}\xi}\right)^2 = 0 \tag{15}$$

with boundary conditions:

$$\left.\begin{aligned} &\xi = 0, \quad \zeta = \frac{\mathrm{d}\zeta}{\mathrm{d}\xi} = 0 \\ &\xi \to \infty, \quad \frac{\mathrm{d}\zeta}{\mathrm{d}\xi} \to 1. \end{aligned}\right\} \tag{16}$$

It should be noted that equation (15) is not the appropriate differential equation when ζ_0 is not zero.

The solution to equation (15) with boundary conditions (16) will be given in Section 3.2.

2.3. *The "similar" b-equation*

The b-equation and the form it takes in similar co-ordinates were discussed in Paper 3, Spalding and Evans [3]. Only a brief statement of the meaning and form of the equation will therefore be given here.

Assuming uniform material properties and using rectangular co-ordinates as in Section 2.1, the two-dimensional laminar boundary-layer equation which expresses the conservation of a fluid property denoted by P is:

$$u\,\frac{\partial P}{\partial x} + v\,\frac{\partial P}{\partial y} = K\,\frac{\partial^2 P}{\partial x^2} \tag{17}$$

where x, y, u and v have been defined in Section 2.1, and

K = a diffusion coefficient; for mass transfer it is the coefficient of diffusion of a mass component in the fluid mixture, for heat transfer it is the thermal diffusivity of the fluid.

Note that the ratio (γ/ρ) appearing in Paper 3 has been replaced by K in equation (17) and in most formulae to be given later in the present paper. In Paper 3, γ was, in fact, defined as the quantity $K\rho$, where ρ is the density of the fluid.

The boundary conditions associated with equation (17) are:

$$\left.\begin{array}{ll}\text{in the main-stream} & P = P_G \\ \text{in the fluid at the interface} & P = P_S\end{array}\right\}. \quad (18)$$

By defining a function of the form:

$$b = \frac{(P - P_S)}{(P_S - P_T)} \quad (19)$$

where:

P_T = value of P in the *transferred substance*, a concept which has been discussed by Spalding [7],

the class of similar solutions to equation (17) being studied in the present work obey the differential equation:

$$b'' + \sigma f b' = 0 \quad (20)$$

with boundary conditions:

$$\left.\begin{array}{ll}\eta = 0, & b = 0 \\ \eta \to \infty, & b \to B\end{array}\right\}. \quad (21)$$

In equation (20) the primes denote differentiation with respect to the independent variable η defined in equation (10) and the Prandtl/Schmidt number σ is:

$$\sigma = \frac{\nu}{K}. \quad (22)$$

In equation (21) the quantity B is:

$$B = \frac{(P_G - P_S)}{(P_S - P_T)}. \quad (23)$$

In addition to the boundary conditions given in equations (21), the condition:

$$b_0' = -\sigma f_0 \quad (24)$$

is also satisfied at the interface, where f_0 is the value of the constant occurring in equation (14).

A short calculation from equation (20) gives for the reciprocal of the group (b'/B) the integral:

$$\left(\frac{B}{b_0'}\right) = \int_0^\infty \exp\left\{-\sigma\int_0^\eta f\,\mathrm{d}\eta\right\}\mathrm{d}\eta. \quad (25)$$

The main purpose of the present paper is to obtain values of the quantity (b_0'/B), often referred to as the "wall gradient", for ranges of values of the parameters β and σ when the constant f_0 is zero. Although the quantities b_0' and B are both zero for this case, their ratio is not since the reciprocal of the integral on the right of equation (25) is the well-known expression for the Nusselt number in similar coordinates, namely:

$$\left(\frac{b_0'}{B}\right) = \frac{(2-\beta)^{1/2}\,Nu}{Re^{1/2}} \quad (26)$$

where the Nusselt number Nu and the Reynolds number Re both have local values.

An expression for the wall gradient (b_0/B) in terms of a "similar" boundary-layer thickness will be given in Section 5.2.

Many other functions of the b-boundary layer can be evaluated when (b_0'/B) is known for fixed values of the parameters β and σ and some of these will be plotted and discussed in Section 7.

3. SOLUTIONS TO THE VELOCITY EQUATION

3.1. *The range* $-0{\cdot}198838 \leqslant \beta \leqslant 2{\cdot}0$

Solutions to equation (13) with boundary conditions (14), to a considerably higher accuracy than those given in Paper 2 and applied in Paper 3a, were quoted recently by Bertram and Feller [8] from work done by Smith [9]. The present author has consulted only Ref. 8. This gave a table of values of the wall gradient f_0'' and the sum $(\delta_1^* + \delta_2^*)$ at fixed values of β in the range $-0{\cdot}198838 \leqslant \beta \leqslant 2{\cdot}0$. The boundary-layer thicknesses δ_1^* and δ_2^* are defined in terms of the similar distance coordinate η as:

$$\delta_1^* = \int_0^\infty \left(1 - \frac{\mathrm{d}f}{\mathrm{d}\eta}\right)\mathrm{d}\eta \quad (27)$$

and

$$\delta_2^* = \int_0^\infty \frac{\mathrm{d}f}{\mathrm{d}\eta}\left(1 - \frac{\mathrm{d}f}{\mathrm{d}\eta}\right)\mathrm{d}\eta. \quad (28)$$

Table 1. Solutions to the velocity equation

β	f_0''	$(\delta_1^* + \delta_2^*)$	δ_2^*	δ_1^*	H_{12}	H_{24}	$\frac{\delta_2^2}{\nu}\frac{du_G}{dx}$	$F_2 \equiv \frac{u_G}{\nu}\frac{d\delta_2^2}{dx}$	E_2
−0·198838	0·0	2·94428	0·58543	2·35885	4·0293	0·0	−0·068147	0·82175	−0·02903
−0·195	0·055172	2·69841	0·58136	2·11705	3·6415	0·032075	−0·065906	0·80777	−0·02662
−0·19	0·08570	2·58328	0·57652	2·00676	3·4808	0·04941	−0·063151	0·79105	−0·02412
−0·18	0·128636	2·43928	0·56771	1·87157	3·2967	0·073028	−0·058013	0·76061	−0·02019
−0·16	0·190780	2·25884	0·55219	1·70665	3·0907	0·10535	−0·048786	0·70740	−0·01459
−0·14	0·239736	2·13446	0·53856	1·59590	2·9633	0·12911	−0·040607	0·66131	−0·01071
−0·10	0·319270	1·95774	0·51504	1·44270	2·8011	0·16444	−0·026527	0·58359	−0·00565
−0·05	0·400323	1·80282	0·49046	1·31236	2·6758	0·19634	−0·012028	0·50518	−0·00206
0·0	0·469600	1·68638	0·46960	1·21678	2·5911	0·22052	0·0	0·44105	0·0
0·05	0·531130	1·59320	0·45147	1·14173	2·5289	0·23979	0·010191	0·38726	0·00120
0·1	0·587035	1·51578	0·43546	1·08032	2·4809	0·25563	0·018963	0·34133	0·00186
0·2	0·686708	1·39239	0·40823	0·98416	2·4108	0·28033	0·033330	0·26664	0·00241
0·3	0·774755	1·29673	0·38574	0·91099	2·3617	0·29885	0·044639	0·20832	0·00237
0·4	0·854421	1·21932	0·36669	0·85263	2·3252	0·31331	0·053785	0·16136	0·00214
0·5	0·927680	1·15482	0·35027	0·80455	2·2969	0·32494	0·061345	0·12269	0·00180
0·6	0·995836	1·09988	0·33591	0·76397	2·2743	0·33451	0·067701	0·090268	0·00142
0·8	1·1202677	1·01053	0·31184	0·69869	2·2405	0·34934	0·077795	0·038898	0·00070
1·0	1·2325877	0·94024	0·29235	0·64789	2·2161	0·36035	0·085469	0·0	0·0
1·2	1·3357215	0·88301	0·27611	0·60690	2·1980	0·36881	0·091484	−0·030495	−0·00055
1·6	1·5215140	0·79443	0·25043	0·54400	2·1723	0·38103	0·10034	−0·075255	−0·00149
2·0	1·6872182	0·72821	0·23080	0·49741	2·1552	0·38941	0·10654	−0·10654	−0·00220
∞†	1·1547005	1·1547005	0·3761614	0·7785391	2·069694	0·4343538	0·1414974	−0·2829948	−0·00614

Except for $\beta = \infty$ columns 2 and 3 evaluated by Smith [9], succeeding columns calculated from these.
† Solutions for $\beta = \infty$ calculated from formula, see Section 3.2.

The values taken from Ref. 8 are given in the first three columns of Table 1. Other functions of the velocity boundary layer which are important in the present series of papers have been calculated from these and are also given in Table 1. The formulae used for evaluating these were:

$$\delta_2^* = f_0'' - \beta(\delta_1^* + \delta_2^*) \tag{29}$$

$$H_{12} = \frac{\delta_1^*}{\delta_2^*} \tag{30}$$

$$H_{24} = f_0'' \, \delta_2^* \tag{31}$$

$$\frac{\delta_2^2}{\nu}\frac{\mathrm{d}u_G}{\mathrm{d}x} = \beta(\delta_2^*)^2 \tag{32}$$

$$F_2 \equiv \frac{u_G}{\nu}\frac{\mathrm{d}\delta_2^2}{\mathrm{d}x} = 2(1-\beta)\,(\delta_2^*)^2. \tag{33}$$

The importance of these functions and their application to the calculation of boundary-layer thicknesses for non-similar flows have been discussed in Paper 1, Spalding [1]. From equation (31) it is clear that the quantity f_0'' could have been written as $1/\delta_4^*$ where δ_4^* is the shear boundary-layer thickness in similar co-ordinates, but this notation is not used here.

The quantity F_2 in equation (33) measures the rate of growth with distance x of the momentum thickness δ_2, and the quantity $(\delta_2^2/\nu)\,(\mathrm{d}u_G/\mathrm{d}x)$ is the corresponding measure of the pressure gradient in the main-stream. It was also shown in Paper 1 that F_2 is very close to being a linear function of $(\delta_2^2/\nu)\,(\mathrm{d}u_G/\mathrm{d}x)$.

Any pair of exact solutions could be chosen so as to obtain the constants in such a linear approximation but it is convenient to choose the points at which F_2 and $(\delta_2^2/\nu)\,(\mathrm{d}u_G/\mathrm{d}x)$ become zero respectively. If this is done with the present exact solutions the following relationship results:

$$F_2 = 0{\cdot}44105 - 5{\cdot}1604\,\frac{\delta_2^2}{\nu}\frac{\mathrm{d}u_G}{\mathrm{d}x} - E_2 \tag{34}$$

where the first two terms on the right represent the linear approximation and the function E_2 is a small correction factor which compensates for the fact that F_2 is not exactly a linear function of $(\delta_2^2/\nu)\,(\mathrm{d}u_G/\mathrm{d}x)$. Values of E_2 are also included in Table 1.

Apart from being more accurate than the values given earlier in Papers 1 and 2 the figures contained in Table 1 cover the region of decelerated flows in greater detail. This may be useful when applying these values since the inaccuracy of the approximate methods discussed in Paper 1 is greatest in this region.

For $\beta \leqslant 2$ most of the original values in columns 2 and 3 of Table 1 are given to six significant digits. In calculating the other functions from these it has been assumed that the last digit given is exact. This generally resulted in an accuracy of five significant digits, although in some cases the last digit is in doubt by up to 5 units. Where doubt existed about particular values, the accuracy retained is at least as high as the original figures allowed.

3.2. *The value* $\beta = \infty$

Table 1 also contains the solution for the case $\beta = \infty$, namely equation (15) with boundary conditions (16). This is one of the few boundary-layer equations whose solution can be obtained in closed form. Only the gradient of ζ with respect to ξ is required here and this is (see Pai [6]):

$$\frac{\mathrm{d}\zeta}{\mathrm{d}\xi} = 3\tanh^2\left\{\frac{\xi}{\sqrt{2}} + \tanh^{-1}\sqrt{\frac{2}{3}}\right\} - 2. \tag{35}$$

From this the gradient at the interface is:

$$\left(\frac{\mathrm{d}^2\zeta}{\mathrm{d}\xi^2}\right)_{\xi=0} = \frac{2}{\sqrt{3}} \tag{36}$$

and the displacement thickness in terms of the similar distance co-ordinate ξ is:

$$\delta_1^* \equiv \int_0^\infty \left(1 - \frac{\mathrm{d}\zeta}{\mathrm{d}\xi}\right)\mathrm{d}\xi = (3\sqrt{2} - 2\sqrt{3}). \tag{37}$$

The momentum boundary-layer thickness may then be evaluated from the relationship:

$$\delta_2^* \equiv \int_0^\infty \left(\frac{\mathrm{d}\zeta}{\mathrm{d}\xi}\right)\left(1 - \frac{\mathrm{d}\zeta}{\mathrm{d}\xi}\right)\mathrm{d}\xi = \left(\frac{\mathrm{d}^2\zeta}{\mathrm{d}\xi^2}\right)_{\xi=0} - \delta_1^* \tag{38}$$

which is deduced from equation (15) by formal integration.

The function H_{12} is then the ratio of (37) to (38), H_{24} is the product of (36) and (38) and the other functions in Table 1 are evaluated from:

$$\frac{\delta_2^2}{\nu}\frac{\mathrm{d}u_G}{\mathrm{d}x} = (\delta_2^*)^2 \tag{39}$$

$$F_2 = 2(\delta_2^*)^2 \tag{40}$$

and E_2 is calculated from equation (34).

Because different similar co-ordinates have been used for the case $\beta = \infty$, functions such as the wall gradient and boundary-layer thicknesses in Table 1 do not form a continuous set with those for other values of β. It should be noted that the wall gradient, which is in fact

$$\left(\frac{d^2\zeta}{d\xi^2}\right)_{\xi=0},$$

has been written in the same column as f''_0. The functions tabulated in the last five columns *do* form a continuous set with the other values, however, since they are independent of the similar co-ordinates used.

The (ζ, ξ) co-ordinates could, of course, have been used throughout but this would have made the formulation of the problem unfamiliar to the reader. It would also have meant treating the case of zero main-stream pressure gradient (when $\beta = 0$ and n is infinite) as an exception.

The values of the functions for $\beta = \infty$ in Table 1 are exact in the last digit.

4. EVALUATING THE WALL GRADIENT (b'_0/B)

4.1. *The general formula*

The methods used for evaluating the integral on the right-hand side of equation (25) have already been described in Papers 3a and 6. In the latter paper it was shown that by dividing the range of integration into two parts, namely $0 \leqslant \eta \leqslant d$ and $d \leqslant \eta \leqslant \infty$, equation (25) may be written:

$$\left.\begin{aligned}\left(\frac{B}{b'_0}\right) = \int_0^d \exp\left\{-\sigma\int_0^\eta f\,d\eta\right\}d\eta \\ + \left(\frac{\pi}{2\sigma}\right)^{1/2}\left\{1 \pm \operatorname{erf}\left[\left(\frac{\sigma}{2}\right)^{1/2} f(d)\right]\right\} \\ \exp\left\{\frac{\sigma}{2}[f(d)]^2 - \sigma\int_0^d f\,d\eta\right\}\end{aligned}\right\} \quad (41)$$

where the sign preceding the error function is opposite to that of $f(d)$; since $f(d)$ is generally positive this is usually negative.

Equation (41) can give high accuracy but only holds when the distance d is large enough. This is so when, at the point $\eta = d$, the shear stress is virtually zero (i.e. f'' is negligibly small) and the stream function f has the value:

$$f = (\eta + f_0 - \delta_1^*). \quad (42)$$

Most of the values of the wall gradient (b'_0/B) to be given later in Table 3 were calculated on a computer. The method has already been described in Paper 6.

4.2. *Asymptotic expansions for high σ*

For very high values of σ the b-boundary layer is very thin and only low values of η contribute significantly to the integral in equation (25) or, in other words, only the first term on the right-hand side of equation (41) is important. Under these circumstances the step-size used for integrating on the computer, namely $\Delta\eta = 0{\cdot}1$, was too large to give high accuracy. For these conditions, therefore, the asymptotic formulae given in Paper 3a were used.

Because very accurate solutions to the velocity equation are now available these formulae have been recalculated. The method by which the asymptotic expansions were obtained is given below in a little more detail than in the earlier paper since this may be useful to someone wishing to make use of the asymptotic expansions.

The stream function f is first expanded in terms of derivatives at the interface giving:

$$f = \frac{f''_0\eta^2}{2!} + \frac{f'''_0\eta^3}{3!} + \frac{f^{\mathrm{IV}}_0\eta^4}{4!} + \frac{f^{\mathrm{V}}_0\eta^5}{5!} + \ldots (43)$$

where the suffix 0 denotes the value at the interface and f_0 has been taken to be zero. Inserting equation (43) into equation (25) and changing the integration variable from η to φ where:

$$\varphi = \left(\frac{\sigma f''_0}{3!}\right)\eta^3 \quad (44)$$

the integral to be evaluated becomes:

$$E = \int_0^\infty e^{-\varphi}\varphi^{-2/3}\exp -\{A_3\varphi^{4/3} + A_5\varphi^{6/3} + A_6\varphi^{7/3} + \ldots\}\,d\varphi. \quad (45)$$

Since the values of σ and f''_0 are known the value of (b'_0/B) may be obtained, if values of E are calculated, by using the relationship:

$$\left(\frac{b'_0}{B}\right) = \frac{3}{E}\left(\frac{\sigma f''_0}{3!}\right)^{1/3}. \quad (46)$$

The coefficients A_r occurring in equation (45) are given by the general formula:

$$A_r = \frac{1}{\sigma^{(r-2)/3}} \frac{f_0^{(r)}}{(r+1)!} \left(\frac{3!}{f_0''}\right)^{(r+1)/3} \quad (47)$$

As was noted in Paper 3a, the coefficients A_0, A_1, and A_4 are zero and A_2 is unity.

The integral E may now be expressed as a series in inverse powers of σ in the following way.

Expanding the second exponential function occurring in the integrand of equation (45) as a power series in φ, each term under the integral sign is of the form $e^{-\varphi} \varphi^{m/3}$, where m has a different value for each term. Using the relationship:

$$\int_0^\infty e^{-\varphi} \varphi^{m/3} \, d\varphi = \Gamma\left(\frac{m+3}{3}\right) \quad (48)$$

where Γ denotes the gamma function, the expression for E may be evaluated term by term. On collecting terms in the same powers of σ the series for E takes the form:

$$E = \Gamma\left(\frac{1}{3}\right) + \sum_{q=1}^{\infty} \frac{a_q}{\sigma^{q/3}}. \quad (49)$$

Using the numerical values $\Gamma(\frac{1}{3}) = 2{\cdot}6789385$, $\Gamma(\frac{2}{3}) = 1{\cdot}3541179$, $\Gamma(1) = 1$ and the abbreviation:

$$D = \frac{\beta}{(f_0'')^{4/3}} \quad (50)$$

the first nine coefficients a_q in equation (49) become:

$$a_1 = 0{\cdot}41009927\text{D} \quad (51)$$

$$a_2 = 0{\cdot}20637046\text{D}^2 \quad (52)$$

$$a_3 = 0{\cdot}14469576\text{D}^3 + 0{\cdot}059531965\ (1 - 2\beta) \quad (53)$$

$$a_4 = 0{\cdot}12182734\text{D}^4 + 0{\cdot}013019024\ (1 - 5\beta)D \quad (54)$$

$$a_5 = 0{\cdot}11608339\text{D}^5 + 0{\cdot}0058962987\ (1 - 12\beta)D^2 \quad (55)$$

$$a_6 = 0{\cdot}12133900\text{D}^6 + 0{\cdot}0018374063\ (1 - 47\beta)D^3 - 0{\cdot}0066146629\ (1 - \beta - 2\beta^2) \quad (56)$$

$$a_7 = 0{\cdot}13651859\text{D}^7 - 0{\cdot}0019337671\ (1 + 58\beta)D^4 - 0{\cdot}43396747 \times 10^{-3}\ (9 - 16\beta - 44\beta^2)D \quad (57)$$

$$a_8 = 0{\cdot}16324225\text{D}^8 - 0{\cdot}0066333360\ (1 + 23\beta)D^5 - 0{\cdot}15315062 \times 10^{-4}\ (296 - 769\beta - 2246\beta^2)D^2 \quad (58)$$

$$a_9 = 0{\cdot}20558658\text{D}^9 - 0{\cdot}013482111\ (1 + 16\beta)D^6 - 0{\cdot}2651380 \times 10^{-6}\ (21{,}893 - 77{,}432\beta - 230{,}158\beta^2)D^3 + 0{\cdot}31180229 \times 10^{-4}\ (23 + 87\beta - 219\beta^2 - 94\beta^3). \quad (59)$$

Numerical values for these nine coefficients for the values of β occurring in Table 1 for which expansion (49) can be used are given in Table 2. To a large extent this table supersedes Table 2 of Paper 3a, except that values of β greater than 2 are not covered in the present table because accurate values of f_0'' were not available. Where differences exist between values given in Paper 3a and the present ones, the latter are to be preferred.

4.3. *The separation point for high σ*

The above series expansions cannot be used for the separation point when $\beta = -0{\cdot}198838$ and $f_0'' = 0$ because the transformation given in equation (44) is invalid. The method for obtaining a series expansion for this case was given fully in Paper 3a and little new can be added here except that the coefficients in the series have been recalculated. The formulae for this case are given under Table 2 where f_0''' has the value $0{\cdot}198838$.

5. TABLE OF VALUES OF (b_0'/B)

5.1. *Discussion of Table 3*

The above methods have been used to evaluate the wall gradient (b_0'/B) for the values of β included in Table 1 and covering a wide range in the parameter σ. The resulting values are given in Table 3. The quantities f_0'' and δ_1^* used in obtaining (b_0'/B) are given at the head of the relevant column.

In each column a broken horizontal line separates values calculated by the computer from those obtained using the asymptotic formula. This means that at that value of σ, which is different for each β, the two methods agreed in the sixth significant digit. It does not mean, however, that the asymptotic series

Table 2. Asymptotic series for high values of σ

β	a_1	a_2	a_3	a_4	a_5	a_6	a_7	a_8	a_9
−0·19	−0·206221 (1)	0·521835 (1)	−0·183164 (2)	0·777685 (2)	−0·372747 (3)	0·172981 (4)	−0·110868 (5)	0·666662 (5)	−0·422203 (6)
−0·18	−0·113678 (1)	0·158572 (1)	−0·300097 (1)	0·712429 (1)	−0·188552 (2)	0·546696 (2)	−0·170588 (3)	0·565593 (3)	−0·197488 (4)
−0·16	−0·597446	0·437992	−0·368806	0·514621	−0·725218	0·110426 (1)	−0·182262 (1)	0·318373 (1)	−0·585242 (1)
−0·14	−0·385513	0·182368	−0·439998 (−1)	0·743308 (−1)	−0·712520 (−1)	0·648830 (−1)	−0·735760 (−1)	0·838712 (−1)	−0·998907 (−1)
−0·10	−0·187937	0·433404 (−1)	0·575125 (−1)	−0·357614 (−2)	0·378000 (−3)	−0·702789 (−2)	0·185046 (−2)	−0·917551 (−3)	0·969692 (−3)
−0·05	−0·694990 (−1)	0·592688 (−2)	0·647809 (−1)	−0·265741 (−2)	0·254623 (−3)	−0·702395 (−2)	0·159993 (−2)	−0·337175 (−4)	0·564096 (−3)
0·0	0·0	0·0	0·595320 (−1)	0·0	0·0	−0·661466 (−2)	0·0	0·0	0·717145 (−3)
0·05	0·476714 (−1)	0·278859 (−2)	0·538061 (−1)	0·115728 (−2)	0·343335 (−4)	−0·625445 (−2)	−0·409445 (−3)	−0·524341 (−4)	0·828017 (−3)
0·1	0·834329 (−1)	0·854168 (−2)	0·488440 (−1)	0·153304 (−2)	−0·295641 (−4)	−0·586955 (−2)	−0·635047 (−3)	−0·127487 (−3)	0·888382 (−3)
0·2	0·135381	0·224896 (−1)	0·409246 (−1)	0·144682 (−2)	−0·444485 (−3)	−0·516077 (−2)	−0·809807 (−3)	−0·209997 (−3)	0·947352 (−3)
0·3	0·172899	0·366819 (−1)	0·346561 (−1)	0·110463 (−2)	−0·117869 (−2)	−0·456198 (−2)	−0·844849 (−3)	−0·162566 (−3)	0·922766 (−3)
0·4	0·202327	0·502315 (−1)	0·292823 (−1)	0·794671 (−3)	−0·206065 (−2)	−0·402983 (−2)	−0·850643 (−3)	−0·230000 (−4)	0·900975 (−3)
0·5	0·226636	0·630269 (−1)	0·244215 (−1)	0·571041 (−3)	−0·302020 (−2)	−0·352110 (−2)	−0·863648 (−3)	0·186415 (−3)	0·859636 (−3)
0·6	0·247432	0·751247 (−1)	0·198739 (−1)	0·434143 (−3)	−0·402652 (−2)	−0·301179 (−2)	−0·896012 (−3)	0·447268 (−3)	0·793330 (−3)
0·8	0·281979	0·975670 (−1)	0·113177 (−1)	0·375330 (−3)	−0·613302 (−2)	−0·189482 (−2)	−0·103174 (−2)	0·109715 (−2)	0·565752 (−3)
1·0	0·310312	0·118159	0·315605 (−2)	0·533001 (−3)	−0·834062 (−2)	−0·613460 (−3)	−0·126440 (−2)	0·189510 (−2)	0·186458 (−3)
1·2	0·334541	0·137331	−0·479662 (−2)	0·793214 (−3)	−0·106437 (−1)	0·872134 (−3)	−0·159744 (−2)	0·282910 (−2)	−0·366851 (−3)
1·6	0·374951	0·172512	−0·203813 (−1)	0·180839 (−2)	−0·155414 (−1)	0·451372 (−2)	−0·256077 (−2)	0·508780 (−2)	−0·206359 (−2)
2·0	0·408342	0·204606	−0·357523 (−1)	0·308343 (−2)	−0·208376 (−1)	0·909301 (−2)	−0·393222 (−2)	0·785809 (−2)	−0·464460 (−2)

The table gives values of the first nine coefficients in the series expansion of the integral E. Values in the table must be multiplied by the powers of ten given in brackets.

$$\text{Formulae: } \left(\frac{b_0'}{B}\right) = \frac{3}{E}\left(\frac{\sigma f_0''}{3!}\right)^{1/3};\ E = 2{\cdot}6789385 + \sum_{q=1}^{\infty} \frac{a_q}{\sigma^{q/3}}.$$

$$\text{When } \beta = -0{\cdot}198838,\ \left(\frac{b_0'}{B}\right) = \frac{4}{E_{\text{sep}}}\left(\frac{\sigma f_0'''}{4!}\right)^{1/4};\ E_{\text{sep}} = 3{\cdot}625610 + \frac{0{\cdot}0840531}{\sigma} - \frac{0{\cdot}00590720}{\sigma^2} - \frac{0{\cdot}000105923}{\sigma^3} + 0(\sigma^{-4}).$$

cannot be used for lower values of σ. Indeed, as was demonstrated in Paper 3a, when β is in the range $-0{\cdot}1 \leqslant \beta \leqslant 2$ as well as for the separation point itself, the series are very useful even when σ is near unity, although the accuracy is lower than for high σ.

The error in the values of (b_0'/B) given in Table 3 is believed to be confined to the sixth significant digit. It is possible for the computing programme to give an error of 5 units in this place but where it was possible to check the values they were found to be correct to within two units in the sixth place. In principle, however, this last place should only be regarded as an estimate of the correct value.

The results for high values of σ, approximately $\sigma \geqslant 10$, for the two columns $\beta = -0{\cdot}19$ and $\beta = -0{\cdot}18$, could contain a greater error than elsewhere because the asymptotic formulae are not very reliable in this region. This may be seen on inspecting the coefficients in Table 2, where no asymptotic formula occurs for $\beta = -0{\cdot}195$.

5.2. *Calculating other functions from (b_0'/B)*

Many other functions associated with the b-boundary layer may be calculated from values of (b_0'/B) for known values of the parameters β and σ. The formulae for doing this are given below, only those applicable to the case $f_0 = 0$ being included; detailed discussion of these formulae was given in Paper 3.

$$\frac{Nu}{Re^{1/2}} = \frac{1}{(2-\beta)^{1/2}}\left(\frac{b_0'}{B}\right) \tag{60}$$

$$\frac{\Delta_2 Re^{1/2}}{x} = \frac{(2-\beta)^{1/2}}{\sigma}\left(\frac{b_0'}{B}\right) \tag{61}$$

$$\frac{\Delta_2}{\Delta_4} = \frac{1}{\sigma}\left(\frac{b_0'}{B}\right)^2 \tag{62}$$

$$\frac{\Delta_4^2}{\nu}\frac{\mathrm{d}u_G}{\mathrm{d}x} = \frac{\beta}{(b_0'/B)^2} \tag{63}$$

$$\frac{u_G}{\nu}\frac{\mathrm{d}\Delta_4^2}{\mathrm{d}x} = \frac{2(1-\beta)}{(b_0'/B)^2} \tag{64}$$

$$\frac{\Delta_2^2}{\nu}\frac{\mathrm{d}u_G}{\mathrm{d}x} = \frac{\beta}{\sigma^2}\left(\frac{b_0'}{B}\right)^2 \tag{65}$$

$$\frac{u_G}{\nu}\frac{\mathrm{d}\Delta_2^2}{\mathrm{d}x} = \frac{2(1-\beta)}{\sigma^2}\left(\frac{b_0'}{B}\right)^2. \tag{66}$$

The quantities X, Y, W and Z considered in earlier papers, which are used in approximate methods of calculating functions in the b-boundary layer when σ is high, are not discussed in the present paper and are therefore omitted from the above list.

When considering the velocity equation in Section 3 above, it was convenient to use boundary-layer thicknesses, written with an asterisk, which were defined in terms of the similar co-ordinate η. In the same way thicknesses associated with the b-boundary layer may be defined as:

$$\Delta_4^* = \Delta_4\left\{\frac{1}{\nu\beta}\frac{\mathrm{d}u_G}{\mathrm{d}x}\right\}^{1/2} \tag{67}$$

and

$$\Delta_2^* = \Delta_2\left\{\frac{1}{\nu\beta}\frac{\mathrm{d}u_G}{\mathrm{d}x}\right\}^{1/2} \tag{68}$$

where Δ_4 and Δ_2 are the conduction and convection boundary-layer thicknesses defined in the notation list in terms of the physical distance y. The present author has found that working in terms of Δ_4^* and Δ_2^* sometimes simplifies formulae and shortens calculations connected with similar boundary layers.

It may be realized why (b_0'/B) is called the "wall gradient" since, on examining equation (67), it is seen to be the reciprocal of Δ_4^*.

6. CALCULATING (b_0'/B) FOR VALUES OF σ OUTSIDE THE RANGE COVERED IN TABLE 3

6.1. *High values*

For most values of β, Table 3 gives good continuous coverage of the Prandtl/Schmidt number up to $\sigma = 100$ but there is a wide gap between this value and $\sigma = 1000$. The procedure for obtaining values for σ greater than 100 is straightforward since only a few terms in the asymptotic series of Table 2 are required. For this reason very high values of σ have not been included in Table 3.

This does not hold, however, for the region approaching but not at the separation point when β has the values $-0{\cdot}195$, $-0{\cdot}19$ and $-0{\cdot}18$. For the first of these no useful asymptotic series could be found, for the second the series given in Table 2 is reasonably accurate only when $\sigma \geqslant 1000$ and for the third accuracy to four significant digits was possible when $\sigma = 100$.

Table 3. *Values of the wall gradient* (b_0'/B) *as a function of the parameter* β *and the fluid property* σ *for* $B = 0$

σ	$\beta =$ −0·198838	−0·195	−0·19	−0·18	−0·16	−0·14	−0·10	−0·05	0·0	0·05	0·10
	$f_0'' =$ 0·0	0·055172	0·08570	0·128636	0·190780	0·239736	0·319270	0·400323	0·469600	0·531130	0·587035
	$\delta_1^* =$ 2·358845	2·117148	2·006757	1·871574	1·706646	1·595900	1·442696	1·312356	1·21678	1·14173	1·080323
0·0001	0·783166(−2)	0·784637(−2)	0·785322(−2)	0·786161(−2)	0·787185(−2)	0·787853(−2)	0·788810(−2)	0·789625(−2)	0·790224(−2)	0·790693(−2)	0·791078(−2)
0·0002	0·109922(−1)	0·110215(−1)	0·110347(−1)	0·110513(−1)	0·110715(−1)	0·110850(−1)	0·111037(−1)	0·111198(−1)	0·111316(−1)	0·111409(−1)	0·111482(−1)
0·0005	0·171249(−1)	0·171961(−1)	0·172284(−1)	0·172686(−1)	0·173178(−1)	0·173510(−1)	0·173967(−1)	0·174361(−1)	0·174650(−1)	0·174877(−1)	0·175064(−1)
0·001	0·238257(−1)	0·239634(−1)	0·240268(−1)	0·241048(−1)	0·242005(−1)	0·242648(−1)	0·243546(−1)	0·244314(−1)	0·244880(−1)	0·245322(−1)	0·245688(−1)
0·002	0·329440(−1)	0·332081(−1)	0·333298(−1)	0·334793(−1)	0·336638(−1)	0·337884(−1)	0·339620(−1)	0·341105(−1)	0·342204(−1)	0·343069(−1)	0·343780(−1)
0·005	0·499082(−1)	0·505154(−1)	0·507968(−1)	0·511445(−1)	0·515736(−1)	0·518647(−1)	0·522712(−1)	0·526213(−1)	0·528805(−1)	0·530852(−1)	0·532532(−1)
0·01	0·674478(−1)	0·685613(−1)	0·690786(−1)	0·697196(−1)	0·705146(−1)	0·710560(−1)	0·718151(−1)	0·724700(−1)	0·729570(−1)	0·733426(−1)	0·736608(−1)
0·02	0·898595(−1)	0·918423(−1)	0·927688(−1)	0·939223(−1)	0·953577(−1)	0·963390(−1)	0·977220(−1)	0·989221(−1)	0·998168(−1)	0·100527	0·101115
0·04	0·117711	0·121128	0·122733	0·124742	0·127255	0·128982	0·131427	0·133562	0·135161	0·136436	0·137494
0·06	0·136662	0·141281	0·143458	0·146189	0·149619	0·151984	0·155342	0·158285	0·160497	0·162265	0·163736
0·08	0·151320	0·156993	0·159675	0·163045	0·167287	0·170219	0·174393	0·178060	0·180821	0·183035	0·184878
0·1	0·163386	0·170009	0·173146	0·177094	0·182073	0·185521	0·190438	0·194766	0·198031	0·200653	0·202839
0·2	0·204776	0·215221	0·220195	0·226481	0·234451	0·240000	0·247957	0·255003	0·260351	0·264665	0·268276
0·3	0·231796	0·245201	0·251602	0·259707	0·270009	0·277199	0·287537	0·296725	0·303712	0·309373	0·314119
0·4	0·252291	0·268186	0·275784	0·285419	0·297680	0·306250	0·318592	0·329584	0·337956	0·344757	0·350465
0·5	0·268990	0·287067	0·295715	0·306686	0·320660	0·330436	0·344529	0·357099	0·366675	0·374482	0·381034
0·6	0·283182	0·303221	0·312813	0·324983	0·340491	0·351347	0·367008	0·380989	0·391675	0·400352	0·407659
0·7	0·295587	0·317422	0·327874	0·341138	0·358045	0·369883	0·386971	0·402236	0·413909	0·423400	0·431396
0·8	0·306646	0·330144	0·341392	0·355667	0·373864	0·386608	0·405011	0·421458	0·434045	0·444280	0·452910
0·9	0·316653	0·341707	0·353698	0·368915	0·388314	0·401901	0·421526	0·439072	0·452504	0·463435	0·472654
1·0	0·325811	0·352331	0·365021	0·381124	0·401650	0·416029	0·436798	0·455372	0·469599	0·481177	0·490949
1·2	0·342142	0·371376	0·385356	0·403091	0·425693	0·441523	0·464392	0·484852	0·500533	0·513301	0·524084
1·4	0·356451	0·388164	0·403321	0·422539	0·447025	0·464170	0·488938	0·511103	0·528095	0·541938	0·553634
1·6	0·369235	0·403245	0·419488	0·440075	0·466292	0·484644	0·511154	0·534878	0·553073	0·567898	0·580430
1·8	0·380825	0·416983	0·434239	0·456100	0·483925	0·503398	0·531521	0·556689	0·575994	0·591728	0·605032
2·0	0·391451	0·429633	0·447841	0·470896	0·500228	0·520748	0·550378	0·576893	0·597234	0·613816	0·627839
2·5	0·414800	0·457612	0·477988	0·503758	0·536503	0·559390	0·592418	0·621968	0·644638	0·663126	0·678768
3·0	0·434776	0·481746	0·504058	0·532244	0·568015	0·592995	0·629022	0·661242	0·685961	0·706124	0·723188
3·5	0·452333	0·503104	0·527179	0·557558	0·596066	0·622934	0·661660	0·696281	0·722840	0·744505	0·762845
4·0	0·468058	0·522351	0·548052	0·580448	0·621468	0·650064	0·691256	0·728067	0·756303	0·779338	0·798840
4·5	0·482344	0·539931	0·567147	0·601418	0·644767	0·674961	0·718432	0·757264	0·787046	0·811342	0·831915
5·0	0·495465	0·556156	0·584794	0·620822	0·666347	0·698034	0·743629	0·784341	0·815561	0·841030	0·862598
6	0·518960	0·585398	0·616656	0·655912	0·705423	0·739836	0·789304	0·833440	0·867277	0·894880	0·918255
7	0·539640	0·611333	0·644974	0·687154	0·740264	0·777133	0·830081	0·877289	0·913470	0·942985	0·967982
8	0·558185	0·634746	0·670583	0·715450	0·771856	0·810968	0·867092	0·917099	0·955414	0·986668	0·101314(1)
9	0·575047	0·656161	0·694042	0·741404	0·800863	0·842048	0·876143	0·953688	0·993968	0·102682(1)	0·105465(1)
10	0·590544	0·675949	0·715748	0·765445	0·827754	0·870872	0·932653	0·987638	0·102974(1)	0·106409(1)	0·109317(1)
15	0·654043	0·758067	0·806104	0·865773	0·940186	0·991478	0·106476(1)	0·112984(1)	0·117962(1)	0·122020(1)	0·125457(1)
20	0·703084	0·822612	0·877411	0·945202	0·102940(1)	0·108272(1)	0·116977(1)	0·124291(1)	0·129881(1)	0·134437(1)	0·138293(1)
25	0·743592	0·876649	0·937284	0·101204(1)	0·110459(1)	0·116805(1)	0·125837(1)	0·133834(1)	0·139941(1)	0·144917(1)	0·149130(1)
30	0·778389	0·923581	0·989401	0·107032(1)	0·117023(1)	0·123859(1)	0·133577(1)	0·142171(1)	0·148732(1)	0·154075(1)	0·158599(1)
40	0·836595	0·100313(1)	0·107796(1)	0·116954(1)	0·128211(1)	0·135890(1)	0·146781(1)	0·156397(1)	0·163731(1)	0·169701(1)	0·174756(1)
50	0·884693	0·106982(1)	0·115242(1)	0·125312(1)	0·137650(1)	0·146043(1)	0·157926(1)	0·168406(1)	0·176393(1)	0·182893(1)	0·188396(1)
100	0·105233(1)	0·130886(1)	0·142053(1)	0·155503(1)	0·171801(1)	0·182810(1)	0·196962(1)	0·211932(1)	0·222291(1)	0·230714(1)	0·237839(1)
1000	0·187172(1)			0·323192(1)	0·362306(1)	0·388169(1)	0·424103(1)	0·455358(1)	0·479006(1)	0·498184(1)	0·514388(1)

Table 3—continued

σ	β = 0·2	0·3	0·4	0·5	0·6	0·8	1·0	1·2	1·6	2·0
	f_0'' = 0·686708	0·774755	0·854421	0·927680	0·995836	1·1202677	1·2325877	1·3357215	1·5215140	1·6872182
	δ_1^* = 0·98416	0·910994	0·852627	0·80455	0·763972	0·698686	0·647892	0·6069005	0·544004	0·497421
0·0001	0·791680(−2)	0·792139(−2)	0·792505(−2)	0·792807(−2)	0·793062(−2)	0·793472(−2)	0·793791(−2)	0·794048(−2)	0·794444(−2)	0·794737(−2)
0·0002	0·111602(−1)	0·111693(−1)	0·111766(−1)	0·111826(−1)	0·111877(−1)	0·111958(−1)	0·112022(−1)	0·112073(−1)	0·112152(−1)	0·112210(−1)
0·0005	0·175354(−1)	0·175578(−1)	0·175757(−1)	0·175904(−1)	0·176029(−1)	0·176227(−1)	0·176384(−1)	0·176511(−1)	0·176706(−1)	0·176851(−1)
0·001	0·246263(−1)	0·246702(−1)	0·247053(−1)	0·247340(−1)	0·247585(−1)	0·247981(−1)	0·248290(−1)	0·248540(−1)	0·248924(−1)	0·249207(−1)
0·002	0·344895(−1)	0·345752(−1)	0·346437(−1)	0·347004(−1)	0·347484(−1)	0·348258(−1)	0·348859(−1)	0·349350(−1)	0·350105(−1)	0·350667(−1)
0·005	0·535192(−1)	0·537230(−1)	0·538866(−1)	0·540221(−1)	0·541364(−1)	0·543224(−1)	0·544679(−1)	0·545860(−1)	0·547683(−1)	0·549039(−1)
0·01	0·741636(−1)	0·745498(−1)	0·748609(−1)	0·751191(−1)	0·753383(−1)	0·756936(−1)	0·759720(−1)	0·761989(−1)	0·765500(−1)	0·768125(−1)
0·02	0·102048	0·102768	0·103348	0·103831	0·104242	0·104910	0·105436	0·105866	0·106531	0·107031
0·04	0·139180	0·140486	0·141544	0·142427	0·143180	0·144409	0·145381	0·146177	0·147417	0·148352
0·06	0·166083	0·167908	0·169391	0·170630	0·171690	0·173423	0·174799	0·175927	0·177691	0·179027
0·08	0·187825	0·190123	0·191992	0·193559	0·194900	0·197099	0·198845	0·200282	0·202534	0·204243
0·1	0·206340	0·209075	0·211303	0·213173	0·214776	0·217408	0·219503	0·221229	0·223940	0·226003
0·2	0·274092	0·278659	0·282402	0·285558	0·288275	0·292761	0·296357	0·299334	0·304045	0·307661
0·3	0·321785	0·327828	0·332796	0·336997	0·340624	0·346633	0·351469	0·355489	0·361880	0·366811
0·4	0·359703	0·367005	0·373020	0·378118	0·382527	0·389852	0·395765	0·400694	0·408558	0·414649
0·5	0·391652	0·400062	0·407003	0·412893	0·417996	0·426490	0·433364	0·439107	0·448292	0·455431
0·6	0·419517	0·428924	0·436697	0·443303	0·449032	0·458584	0·466329	0·472813	0·483206	0·491305
0·7	0·444384	0·454700	0·463233	0·470493	0·476796	0·487319	0·495865	0·503031	0·514539	0·523528
0·8	0·466940	0·478094	0·487330	0·495195	0·502028	0·513450	0·522741	0·530540	0·543087	0·552908
0·9	0·487652	0·499586	0·509477	0·517905	0·525234	0·537495	0·547482	0·555875	0·569396	0·579999
1·0	0·506854	0·519519	0·530022	0·538979	0·546773	0·559823	0·570466	0·579417	0·593859	0·605200
1·2	0·541651	0·555657	0·567287	0·577216	0·585864	0·600368	0·612217	0·622202	0·638345	0·651058
1·4	0·572702	0·587920	0·600568	0·611376	0·620798	0·636620	0·649567	0·660491	0·678187	0·692154
1·6	0·600872	0·617199	0·630780	0·642393	0·652526	0·669558	0·683513	0·695302	0·714430	0·729556
1·8	0·626744	0·644097	0·658541	0·670901	0·681692	0·699846	0·714737	0·727329	0·747789	0·763995
2·0	0·650735	0·669045	0·684294	0·697350	0·708756	0·727957	0·743722	0·757067	0·778775	0·795995
2·5	0·704326	0·724788	0·741848	0·756472	0·769261	0·790824	0·808565	0·823608	0·848141	0·867660
3·0	0·751084	0·773436	0·792089	0·808091	0·822097	0·845740	0·865224	0·881766	0·908797	0·930356
3·5	0·792839	0·816887	0·836968	0·854207	0·869305	0·894819	0·915867	0·933761	0·963045	0·986445
4·0	0·830744	0·856336	0·877718	0·896084	0·912179	0·939396	0·961870	0·981001	0·101234(1)	0·103743(1)
4·5	0·865578	0·892593	0·915174	0·934578	0·951591	0·980379	0·100417(1)	0·102444(1)	0·105768(1)	0·108433(1)
5·0	0·897897	0·926233	0·949928	0·970298	0·988164	0·101841(1)	0·104343(1)	0·106476(1)	0·109978(1)	0·112787(1)
6	0·956529	0·987268	0·101299(1)	0·103511(1)	0·105453(1)	0·108744(1)	0·111469(1)	0·113794(1)	0·117618(1)	0·120693(1)
7	0·100890(1)	0·104181(1)	0·106934(1)	0·109303(1)	0·111384(1)	0·114912(1)	0·117838(1)	0·120336(1)	0·124449(1)	0·127761(1)
8	0·105651(1)	0·109133(1)	0·112049(1)	0·114564(1)	0·115549(1)	0·120516(1)	0·123623(1)	0·126279(1)	0·130655(1)	0·134185(1)
9	0·110024(1)	0·113687(1)	0·116757(1)	0·119400(1)	0·121724(1)	0·125668(1)	0·128942(1)	0·131743(1)	0·136363(1)	0·140092(1)
10	0·114083(1)	0·117913(1)	0·121123(1)	0·123889(1)	0·126320(1)	0·130450(1)	0·133880(1)	0·136815(1)	0·141660(1)	0·145575(1)
15	0·131088(1)	0·135621(1)	0·139421(1)	0·142699(1)	0·145582(1)	0·150488(1)	0·154570(1)	0·158071(1)	0·163864(1)	0·168560(1)
20	0·144623(1)	0·149706(1)	0·153976(1)	0·157661(1)	0·160905(1)	0·166428(1)	0·171030(1)	0·174980(1)	0·181529(1)	0·186848(1)
25	0·156035(1)	0·161595(1)	0·166262(1)	0·170290(1)	0·173838(1)	0·179882(1)	0·184923(1)	0·189253(1)	0·196439(1)	0·202284(1)
30	0·166013(1)	0·171984(1)	0·176997(1)	0·181326(1)	0·185139(1)	0·191639(1)	0·197063(1)	0·201725(1)	0·209469(1)	0·215774(1)
40	0·183039(1)	0·189711(1)	0·195315(1)	0·200156(1)	0·204420(1)	0·211699(1)	0·217776(1)	0·223004(1)	0·231699(1)	0·238789(1)
50	0·197413(1)	0·204677(1)	0·210779(1)	0·216052(1)	0·220701(1)	0·228633(1)	0·235262(1)	0·240960(1)	0·250464(1)	0·258218(1)
100	0·249515(1)	0·258923(1)	0·266816(1)	0·273669(1)	0·279702(1)	0·290007(1)	0·298633(1)	0·306069(1)	0·318473(1)	0·328625(1)
1000	0·540920(1)	0·562304(1)	0·580290(1)	0·595859(1)	0·609613(1)	0·633154(1)	0·652914(1)	0·669990(1)	0·698593(1)	0·722117(1)

Values given in the table must be multiplied by the powers of ten given in brackets.
Values above broken lines calculated by a computer, those below the lines calculated from an asymptotic formula.

6.2. *Low values*

When $\sigma \leqslant 0{\cdot}0001$ the wall gradient (b_0'/B) may be obtained to good accuracy by taking the first term on the right-hand side of equation (41) to be equal to the distance d and evaluating the second term from suitable values of the functions $f(d)$ and $\int^0 f\,\mathrm{d}\eta$ obtained from solutions to the velocity equation. These quantities and the formula to be used are given in Table 4.

Table 4. *Functions for evaluating* (b_0'/B) *when* $\sigma \leqslant 0{\cdot}0001$

Formula:

$$\left(\frac{B}{b_0'}\right) = d + \left(\frac{\pi}{2\sigma}\right)^{1/2}\left\{1 - \operatorname{erf}\left(\frac{\sigma}{2}\right)^{1/2} f(d)\right\} \exp\left\{\frac{\sigma}{2}\left[f(d)\right]^2 - \sigma\int_0^d f\,\mathrm{d}\eta\right\}$$

β	d	$f(d)$	$\int_0^d f\,\mathrm{d}\eta$
−0·198838	5·4	3·04164	5·15335
−0·195	5·4	3·28316	5·91030
−0·19	5·4	3·39337	6·26970
−0·18	4·8	2·92909	4·78499
−0·16	4·8	3·09371	5·25598
−0·14	4·8	3·20432	5·58319
−0·10	4·8	3·35742	6·05042
−0·05	4·2	2·88817	4·54870
0·0	6·2	4·98322	12·7674
0·05	4·2	3·05849	5·00374
0·10	4·2	3·11984	5·17306
0·2	4·2	3·21593	5·44433
0·3	3·6	2·68948	3·86245
0·4	3·6	2·74768	3·99968
0·5	3·6	2·79567	4·11511
0·6	3·6	2·83618	4·21423
0·8	3·6	2·90141	4·37722
1·0	3·6	2·95216	4·50708
1·2	3·0	2·39341	2·99810
1·6	3·0	2·45616	3·12827
2·0	3·0	2·50273	3·22789

For $\sigma = 0{\cdot}0001$ this agrees with the values given in Table 3 by better than three units in the fifth significant digit. For smaller σ the accuracy would be better. It should be noted that using the value $f(d) = (d - \delta_1^*)$, instead of the values of $f(d)$ listed in Table 4, slightly improves the agreement with computed values at $\sigma = 0{\cdot}0001$.

7. CURVES OF FUNCTIONS OF THE *b*-BOUNDARY LAYER

7.1. *General discussion*

Many functions relating to the *b*-boundary layer can be plotted from the results contained in Table 3. Some functions which are useful in the general methods of boundary-layer calculation mentioned in Section 1.1 will be discussed in the present section.

If δ represents a boundary-layer thickness relating to the velocity boundary layer, it was seen in Papers 1 and 2 that in order to apply some of these general methods, it was necessary to know how the function $(u_G/\nu)\,(\mathrm{d}\delta^2/\mathrm{d}x)$ varied with $(\delta^2/\nu)\,(\mathrm{d}u_G/\mathrm{d}x)$. The first of these is a measure of the rate of growth of δ with distance x and the second is the corresponding measure of the main-stream pressure gradient.

In plotting these relationships for the *b*-boundary layer when the parameter σ was small, it was found necessary to multiply the functions by σ in order to bring closer together curves for a wide range of σ. If Δ is the relevant boundary-layer thickness, this means that the functions are in fact $(u_G/K)\,(\mathrm{d}\Delta^2/\mathrm{d}x)$ and $(\Delta^2/K)\,(\mathrm{d}u_G/\mathrm{d}x)$, where K is the thermal diffusivity for heat transfer or the diffusion coefficient for mass transfer. This form of the functions is not surprising when it is realized, on comparing equations (1) and (17), that K plays the same role in the *b*-boundary layer as does ν in the velocity layer.

The forms of these relationships are, of course, obtained from exact similar solutions to the boundary-layer equations. An important assumption underlying much of the present work is that these relationships, once established, are quite generally valid and can therefore be used to estimate boundary-layer thicknesses and transfer rates for any uniform property, laminar boundary layer.

The relationships for large values of σ were discussed in Paper 3a. The present results are more accurate than those given earlier but the difference is too small to be seen even when the figures are drawn to a large scale. The reader is therefore referred to Paper 3a for a more detailed discussion of the case of large σ. The region of decelerated flow in the range $-0{\cdot}198838 \leqslant \beta \leqslant -0{\cdot}1$ was not adequately

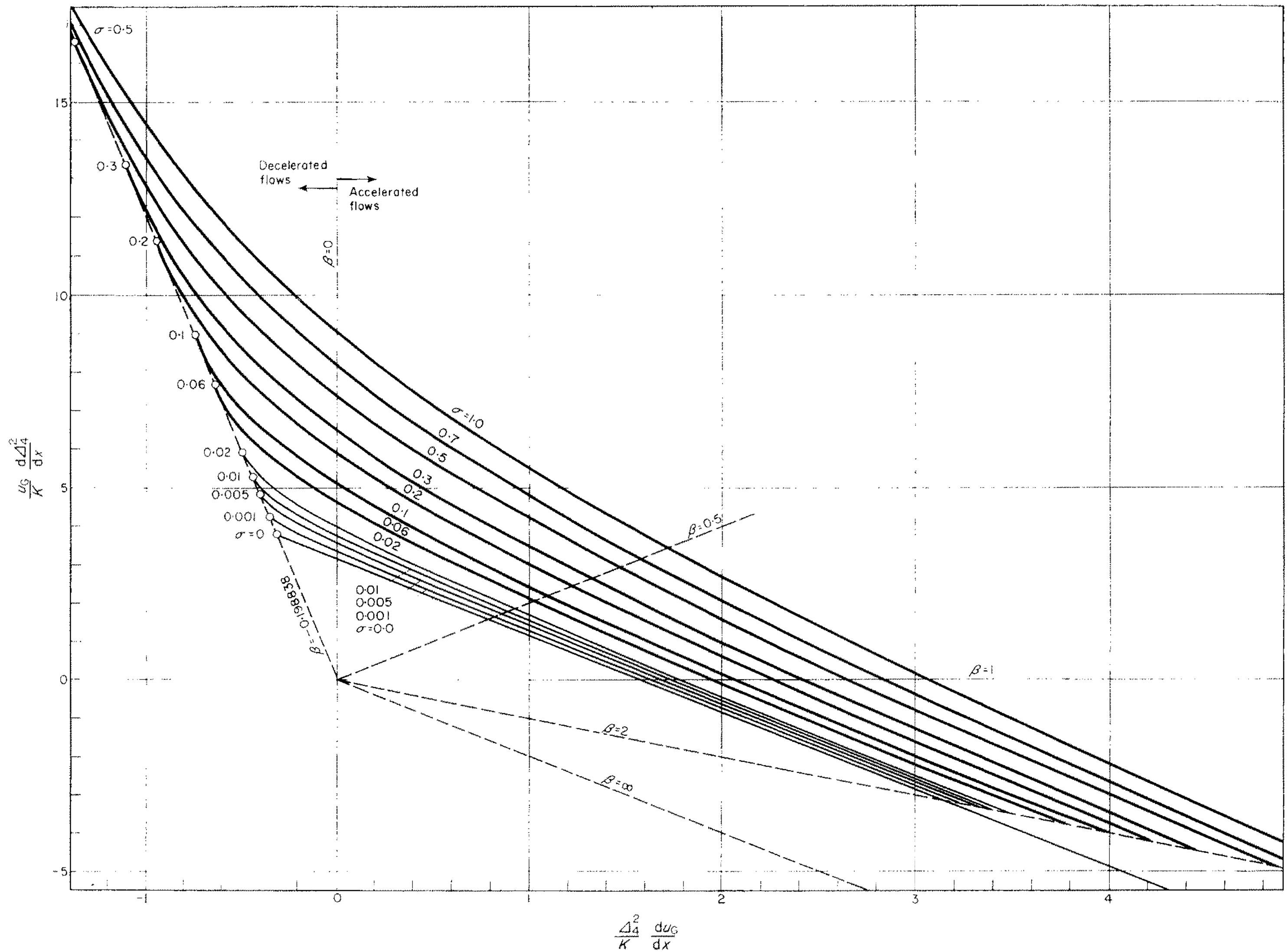

FIG. 1. Variation of the rate of growth with distance x of the conduction thickness Δ_4, expressed by the function $(u_G/K)(d\Delta_4/dx)$, with the main-stream pressure gradient, expressed by $(\Delta_4^2/K)(du_G/dx)$, for low values of the Prandtl/Schmidt number σ. Separation points are indicated by circles.

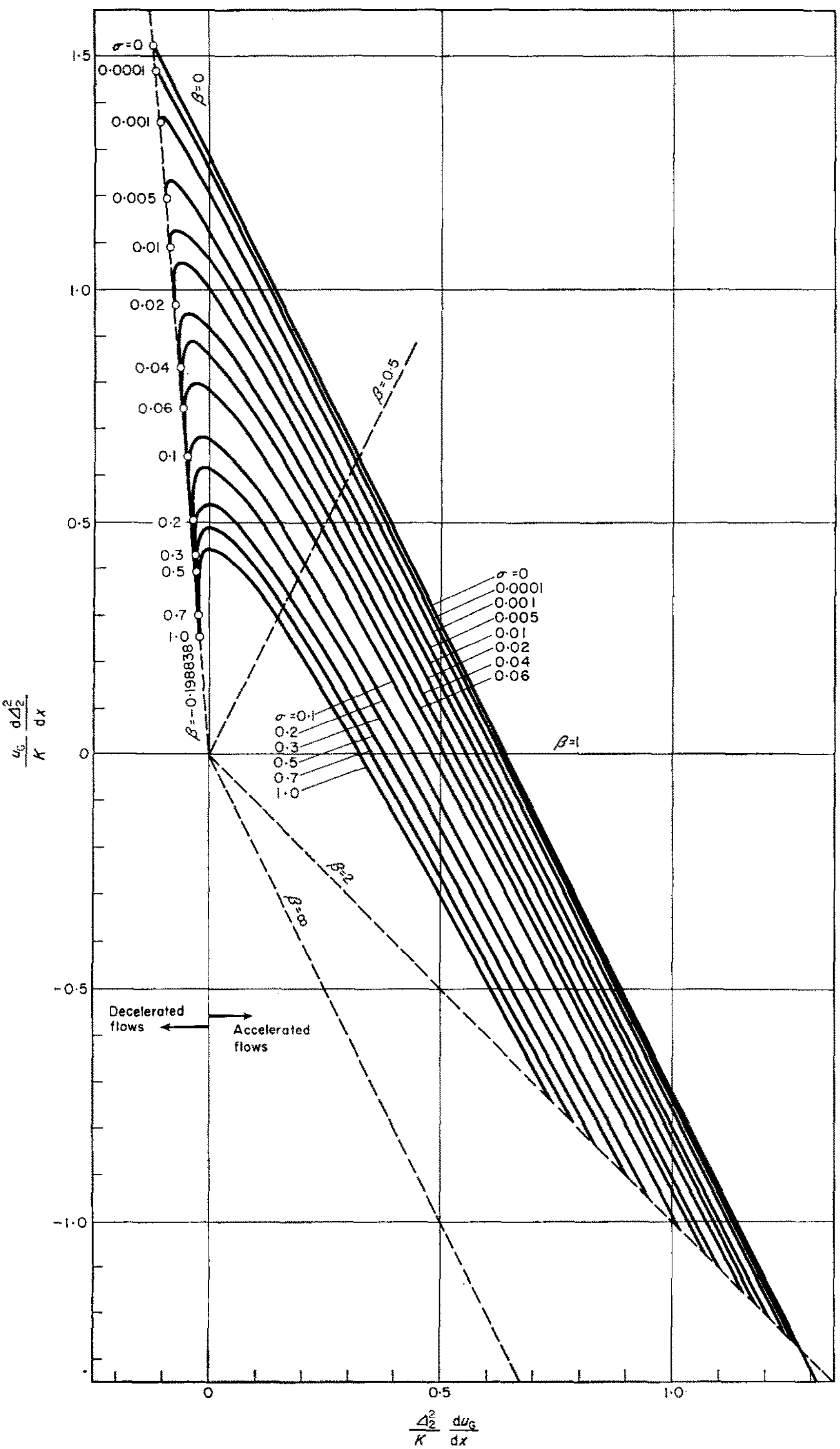

FIG. 2. The same relationship as in Fig. 1 but relating to the convection thickness Δ_2; separation points again indicated by circles.

covered in that earlier paper, however, and figures for this will be discussed below.

7.2. *The conduction thickness for low σ*

Figure 1 applies to the conduction thickness Δ_4 and covers the range in σ from 0 to 1·0. Although curves are not included for all values of σ contained in Table 3, interpolation for intermediate values is straightforward.

When σ is small the wall gradient (b_0'/B) is almost proportional to $\sigma^{1/2}$, and for very small σ it tends to the value $(2\sigma/\pi)^{1/2}$. Inserting this last value into equations (63) and (64) and eliminating β between them gives for the line $\sigma = 0$ in Fig. 1, the equation:

$$\frac{u_G}{K}\frac{d\Delta_4^2}{dx} = \pi - 2\frac{\Delta_4^2}{K}\frac{du_G}{dx} \tag{69}$$

a straight line of slope -2 cutting the abscissa at $\pi/2$ and the ordinate at π. The point marked as the separation point for this line is merely its intersection with the line for $\beta = -0{\cdot}198838$; it has the co-ordinates $(-0{\cdot}0994195\,\pi, 0{\cdot}801162\,\pi)$.

The line given by equation (69) can be interpreted as that applicable to inviscid flow when ν is zero, as well as the limiting case when, although ν is not small, K has a very large value. In either of these cases the velocity boundary layer has a negligible effect. The displacement of any other curve from this line is then a measure of the amount by which the velocity boundary layer affects transfer rates; this displacement is then greater and the curvature more pronounced in regions of decelerated flows where the velocity layer is thick. In spite of this curvature, which increased with increasing σ, these curves would be considerably easier to apply than those for high σ discussed in Paper 3a.

As main-stream acceleration increases each curve approaches the line for $\sigma = 0$ and the slope tends to the value -2 from below. Since the line for $\beta = \infty$ has exactly this slope it appears that no solution for this case occurs on this figure when plotted in this way.

7.3. *The convection thickness for low σ*

The relationship for the convection thickness Δ_2 is shown in Fig. 2.

On this figure the straight line for $\sigma = 0$ is readily shown to be:

$$\frac{u_G}{K}\frac{d\Delta_2^2}{dx} = \frac{4}{\pi} - 2\frac{\Delta_2^2}{K}\frac{du_G}{dx} \tag{70}$$

again a straight line of slope -2 but this time cutting the abscissa at $2/\pi$ and the ordinate at $4/\pi$. The separation point for this line has the co-ordinates $(-0{\cdot}397676/\pi, 3{\cdot}204648/\pi)$.

The remarks made about Fig. 1 in the preceding section apply also to Fig. 2 with obvious modification where necessary.

7.4. *Variation of the ratio (Δ_2/Δ_4) with pressure gradient*

When considering the velocity boundary layer it was shown in Figs. 4(a) and (b) of Paper 2 how the ratio of boundary-layer thicknesses H_{24} $(=\delta_2/\delta_4)$ varied with the pressure gradient parameter $(\delta_2^2/\nu)\,(du_G/dx)$. Figs. 3 and 4 of the present paper show the analogous relationship for the b-boundary layer; Fig. 3 covers the range of low σ from 0 to 2·0 and Fig. 4 high values from 1 to infinity. In Fig. 3 the pressure gradient parameter plotted along the abscissa is $(\Delta_2^2/K)\,(du_G/dx)$.

On this figure "similar" solutions, namely those for a fixed value of β, may be shown by eliminating (b_0'/B) between equations (62) and (65), to be of the form:

$$\frac{\Delta_2}{\Delta_4} = \frac{1}{\beta}\frac{\Delta_2^2}{K}\frac{du_G}{dx} \tag{71}$$

a straight line of slope $1/\beta$ passing through the origin. A few of these lines are shown in the figure. From equation (62) it may also be shown that Δ_2/Δ_4 has the value $2/\pi$ when σ is zero whatever the pressure gradient in the main-stream.

The corresponding curves for high values of σ are plotted in Fig. 4 where the functions used for Fig. 3 have been multiplied by $\sigma^{1/3}$ in order to bring curves for a wide range of σ close together. This multiplying factor is effective for accelerated and slightly decelerated flows where the wall gradient (b_0'/B) is proportional to $\sigma^{1/3}$ for large σ. For decelerated flows approaching separation conditions, however, it is not so useful because, since (b_0'/B) is then proportional to $\sigma^{1/4}$ for large σ, the point for $\sigma = \infty$ is at the origin.

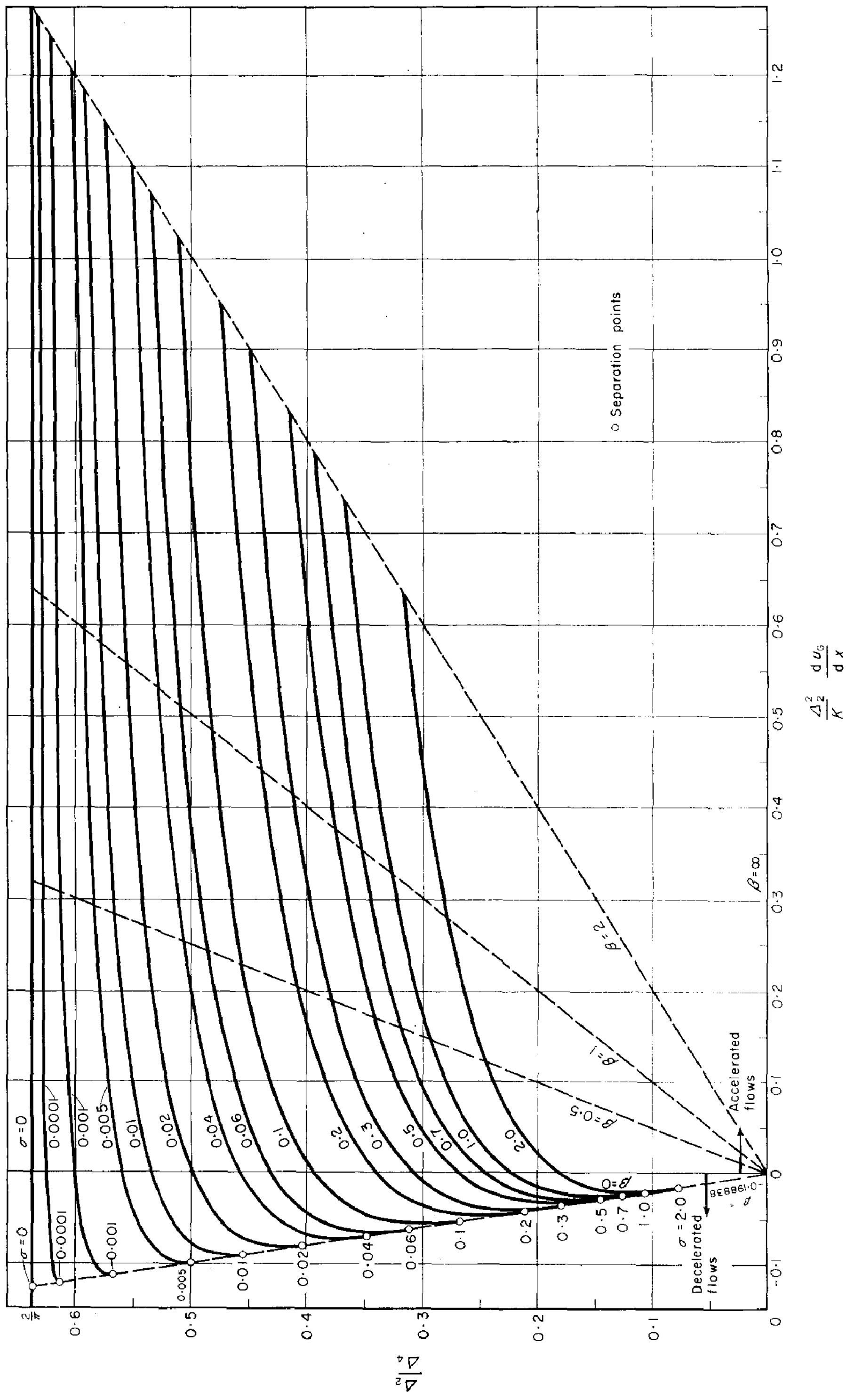

FIG. 3. Variation of the ratio of boundary-layer thicknesses (Δ_2/Δ_4) with main-stream pressure gradient, expressed by $(\Delta_2^2/K)\,(du_G/dx)$, for low values of the Prandtl/Schmidt number σ.

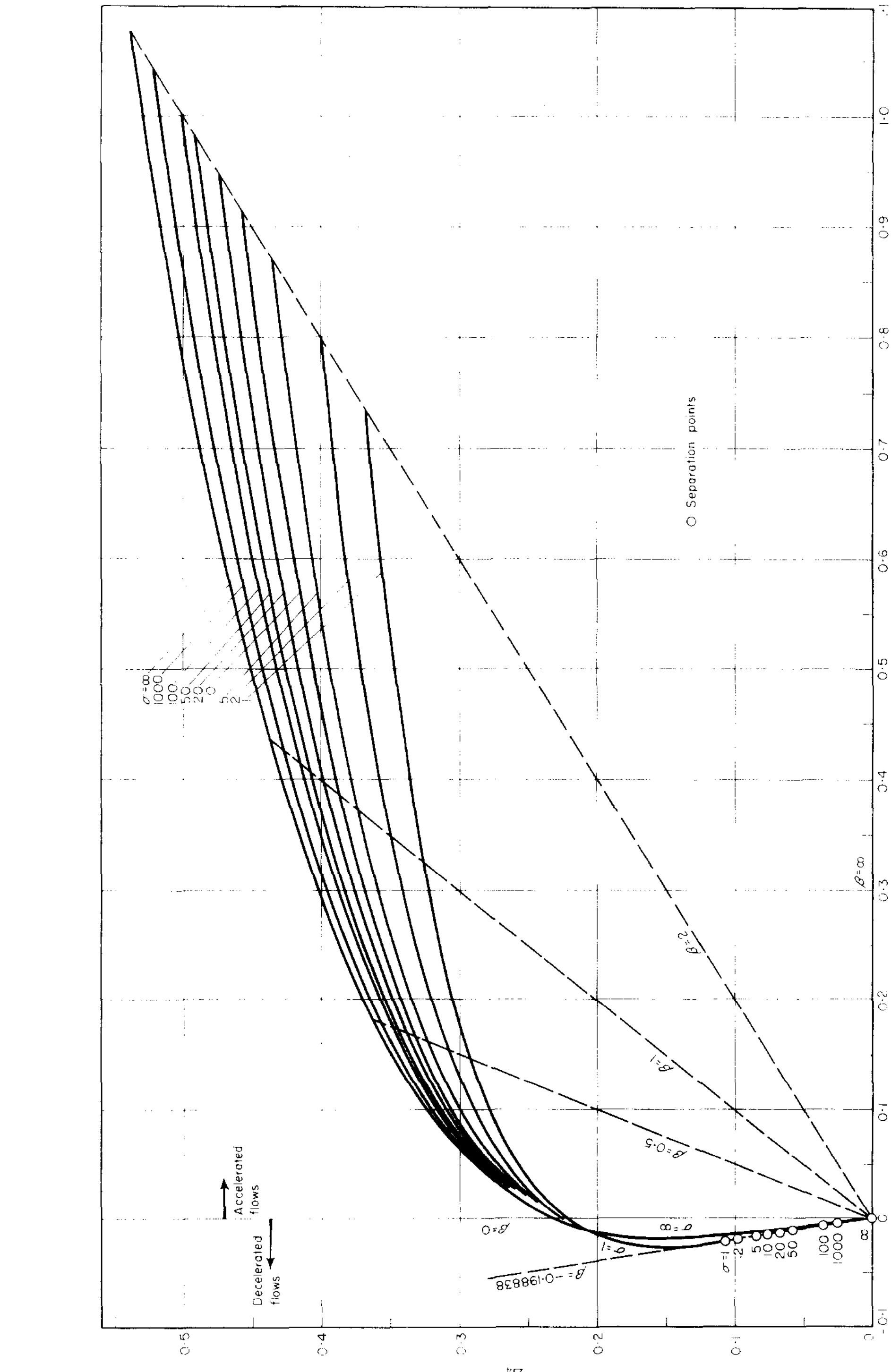

FIG. 4. The same relationship as in Fig. 3 but for high values of the Prandtl/Schmidt number σ. The multiplying factor $\sigma^{1/3}$ merely brings curves for a wide range of σ close together.

7.5. *Decelerated flow and high σ*

Figures 5 and 6 give relationships for decelerated flows and high values of σ which could not be adequately treated in Paper 3a because accurate solutions to the velocity equation were not known.

Figure 5, which refers to the conduction thickness Δ_4, has co-ordinates appropriate to the case when the wall gradient (b_0'/B) is proportional to $\sigma^{1/3}$. Because they are so close together curves for only a few values of σ are given. That for $\sigma = 1000$ has been stopped at $\beta = -0{\cdot}19$ as no asymptotic formula could be found for $\beta = -0{\cdot}195$. The slopes of the curves in this region must be close to that for the line $\beta = -0{\cdot}198838$, that for $\sigma = \infty$ eventually having exactly that slope as it must meet this line at infinity.

Figure 6 refers to the convection thickness Δ_2 and is an improved version of Fig. 2(b) of Paper 3a. In that earlier figure the curves were drawn so that separation points for the range of values of σ were close together. In Fig 6 curves for slightly decelerated flows are close together but the separation points are far apart. Some of the curves have been omitted in the region between $\beta = 0$ and $\beta = -0{\cdot}1$ where they are close together and intersect.

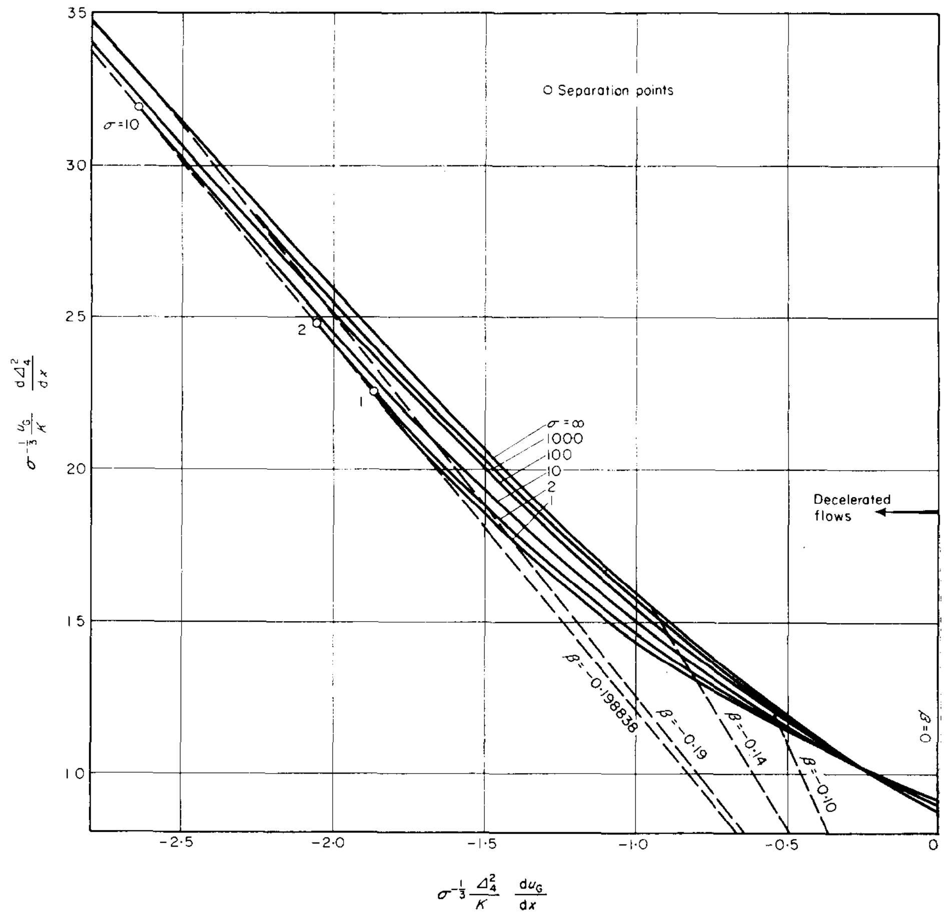

FIG. 5. The same relationship as in Fig. 1 but for decelerated flows and high values of σ. The multiplying factor $\sigma^{-1/3}$ brings curves for a wide range of σ close together.

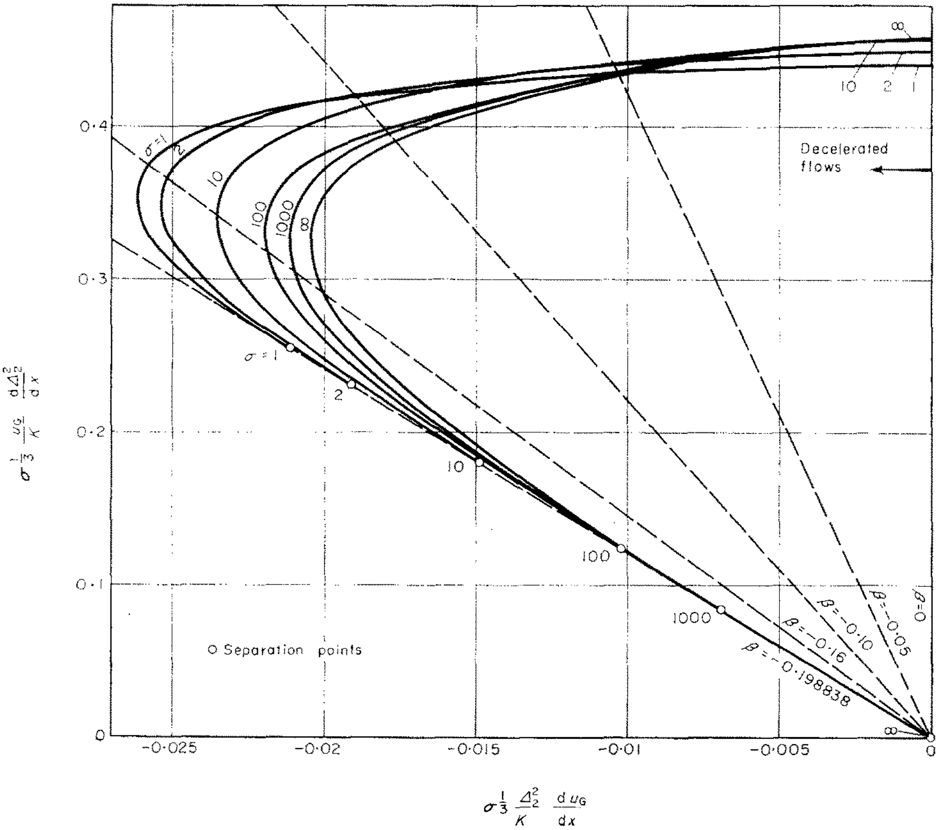

FIG. 6. The same relationship as in Fig. 5 but for the convection thickness Δ_2.

ACKNOWLEDGEMENTS

The present work forms part of the research programme of the Division of Food Preservation, C.S.I.R.O., Australia. The author is grateful to the staff of the Adolph Basser Computing Laboratory, University of Sydney, who computed most of the values contained in Table 3. He would also like to express his gratitude to Miss J. D. Hayhurst, who calculated the other values and prepared the tables and figures.

REFERENCES

1. D. B. SPALDING, Mass transfer through laminar boundary layers—1. The velocity boundary layer. *Int. J. Heat Mass Transfer*, **2**, Nos. 1/2, 15 (1961). Referred to as Paper 1.
2. D. B. SPALDING and H. L. EVANS, Mass transfer through laminar boundary layers—2. Auxiliary functions for the velocity boundary layer. *Int. J. Heat Mass Transfer*, **2**, No. 3, 199 (1961). Referred to as Paper 2.
3. D. B. SPALDING and H. L. EVANS, Mass transfer through laminar boundary layers—3. Similar solutions to the *b*-equation. *Int. J. Heat Mass Transfer*, **2**, No. 4, 314 (1961). Referred to as Paper 3.
4. H. L. EVANS, Mass transfer through laminar boundary layers—3a. Similar solutions to the *b*-equation when $B = 0$ and $\sigma \geqslant 0{\cdot}5$. *Int. J. Heat Mass Transfer*, **3**, No. 1, 26 (1961). Referred to as Paper 3a.
5. H. L. EVANS, Mass transfer through laminar boundary layers—6. Methods of evaluating the wall gradient (b_0'/B) for similar solutions; some new values for zero main-stream pressure gradient. *Int. J. Heat Mass Transfer*, **3**, No. 4, 321 (1961). Referred to as Paper 6.
6. SHIH-I PAI, *Viscous Flow Theory—I. Laminar Flow*, p. 182. Van Nostrand, Princeton (1956).
7. D. B. SPALDING, A standard formulation of the steady convective mass transfer problem. *Int. J. Heat Mass Transfer*, **1**, Nos. 2/3, 192 (1960).
8. M. H. BERTRAM and W. V. FELLER, A simple method

of determining heat transfer, skin friction and boundary layer thickness for hypersonic laminar boundary-layer flows in a pressure gradient. *NASA* Memo. 5-24-59L (1959).

9. A. M. O. SMITH, *Improved Solutions of the Falkner and Skan Boundary Layer Equations.* Rep. E.S. 16009 (Contract No. NOa(s)9027), Douglas Aircraft Co. Inc., Mar. 31 (1952).

Résumé—Cet article concerne l'étude des écoulements à uniformes à couche limite laminaire avec transport de masse à la paroi. Dans ce cas, des solutions semblables de l'équation dynamique ont déjà été données; elles conduisent à une grande précision et couvrent un domaine d'écoulements principaux décélérés et modérément accélérés. Les solutions sont tout d'abord exprimées sous la forme adoptée dans les premiers articles de cette série et sont ensuite utilisées pour l'évaluation du gradient à la paroi pour la couche limite-b (c'est-à-dire, nombre de Nusselt en coordonnées adimensionnelles). Les développements en série donnant ce gradient à la paroi, quand le nombre de Prandtl/Schmidt est grand, présentés dans l'article 3(a), ont été recalculés pour en améliorer la précision. Une table des valeurs du gradient à laparoi couvre le domaine des σ compris entre 0,0001 et 1000; en dehors de ce domaine, il peut être rapidement calculé. Quelques fonctions obtenues à partir de ce gradient à la paroi ont été représentées graphiquement et sont discutées.

Zusammenfassung—Es wird über laminare Grenzschichtströmungen mit einheitlichen Stoffeigenschaften berichtet, für den Fall, dass kein Stofftransport durch die Grenzflächen auftritt. Ähnlichkeitslösungen grosser Genauigkeit sind dafür in der Literatur für den Bereich verzögerter bis schwach beschleunigter Hauptströmungen angegeben. Die Lösungen wurden erst in die Form gebracht, wie sie in früheren Arbeiten dieser Reihe verwendet war, um dann damit den Wandgradienten für die b-Grenzschicht (d.h. die Nusseltzahl in Ähnlichkeitskoordinaten) zu errechnen. Die Reihenentwicklungen für den Wandgradienten bei grosser Prandtl/Schmidtzahl σ, die schon in der Arbeit 3(a) angegeben sind, wurden in der Genauigkeit gesteigert. Eine Tabelle für die Werte des Wandgradienten umfasst σ von 0,0001 bis 1000, wobei für beide Richtungen ausserhalb dieses Bereiches Berechnungen möglich sind. Einige aus dem Wandgradienten erhaltene Funktionen werden aufgezeichnet und diskutiert.

Аннотация—В настоящей статье рассматривается течение ламинарного пограничного слоя с постоянными физическими характеристиками. В случае, когда масса не проходит через границу раздела. В литературе для данного случая были найдены подобные решения для уравнения движения; эти решения даны с большой точностью для ускоренных и замедленных внешних потоков. Сначала решения приведены в том виде, в каком они даны в первых статьях настоящей серии, а затем использованы для вычисления градиента на стенке для b-пограничного слоя (т.е. критерий Нуссельта в координатах подобия). Для уточнения был произведен перерасчёт разложений в ряд с целью получения градиента на стенка при большом значении критерия Прандтля-Шмидта σ, приведенном в статье 3(а). Таблица значений градиента на стенке включает значения σ от 0·0001 до 1000; этот градиент на стенке может быть легко вычислен и за пределами этого диапазона, Даны графически и проанализированы некоторые функции, полученные при определении градиента на стенке.